Field Experiences With a Highly Unbalanced Magnetically Suspended Flywheel Rotor

Markus Ahrens
International Center for Magnetic Bearings, ETH Zurich, Switzerland

Ladislav Kučera
International Center for Magnetic Bearings, ETH Zurich, Switzerland

René Larsonneur
MECOS Traxler AG, Winterthur, Switzerland

Abstract: This paper describes the behaviour of a highly unbalanced flywheel rotor. The unbalance leads to rotational synchronous harmonic bearing forces which may cause amplifier saturation. It will be shown that the balancing of the rotor can be achieved with data obtained from the magnetic bearings. Additionally, it will be shown that the housing dynamics can have an enormous influence on the balancing data. Furthermore, experiences with unbalance compensation are given. The results presented in this paper show that the rotor does not, as often written, rotate "force-free" and therefore does not spin around its principal axis of inertia. Moreover, for rotors with high gyroscopic coupling an undamped resonance occurs. In this frequency range it is impossible to use unbalance compensation. The results presented in this paper are crucial for magnetic bearing systems and have to be considered in their design.

Nomenclature

$\boldsymbol{a}$ (bold letter)	complex value
$\boldsymbol{A}$ (bold capital letter)	matrix

$\boldsymbol{x}_e$	eccentricity
$\boldsymbol{x}_r$	rotor displacement
$\boldsymbol{x}_g$	housing displacement
$\boldsymbol{i}$	magnetic bearing current
$\boldsymbol{F}_m$	magnetic bearing force
$\boldsymbol{F}_g$	force between housing and foundation
$\boldsymbol{F}_u$	unbalance force
k_s	force-displacement factor
k_i	current-displacement factor
k_g	stiffness of housing suspension
d_g	damping of housing suspension
m_r	mass of the rotor
m_g	mass of the housing
J_{rx}	moment of inertia of the rotor about the x-axis
J_{rz}	moment of inertia of the rotor about the z-axis
J_{gx}	moment of inertia of the housing about the x-axis
j	imaginary number
Ω	rotational speed
t	time

Indices

a	bearing plane a
b	bearing plane b
x	x-direction
y	y-direction

1 Introduction

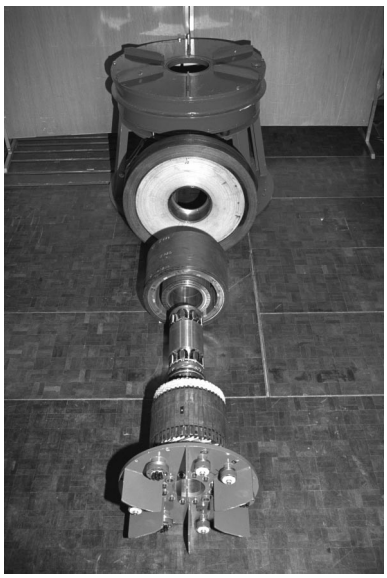

Figure 1: The kinetic energy storage system KIS
From above: housing, flywheel, rotor, stator of the radial magnetic bearings, stator of the electrical machine.

A flywheel energy storage device ("Kinetic Energy Storage, KIS") with high power (250 kW) and 1 kWh of usable energy has been developed at ETH[1]. It is designed for levelling peaks in the power consumption of seam-welding machines. The system consists of a composite fibre-reinforced high speed flywheel, a high speed mo-

[1]The project was funded by NEFF (Nationaler Energie Forschungs-Fond).
Project partners are the Institute of Electrical Machines and the Chair of Power Electronics and Electrometrology.

tor/generator, high efficiency power electronics and an inner type stator with active magnetic bearings (AMB) (see figure 1).

The composite flywheel is connected to the outer type rotor with a cone interference fit. A synchronous motor with lamination sheets on the inner rotor and permanent magnets mounted on lamination sheets on the outer rotor is used. Due to the manufacturing process of the composite flywheel, the interconnection between the flywheel and rotor as well as due to the lamination sheets mounted on the rotor, a high level of unbalance is created which leads to rotational synchronous harmonic forces in the bearings. These unbalance forces increase with the square of the rotational speed, such that the necessary AMB control current may exceed its maximum value. Therefore, unbalance effects can limit the maximum rotational speed.

Usually neither the location nor the magnitude of the rotor unbalance are known. If the rotor is assumed as rigid it is sufficient to measure the excitations in two radial bearing planes in order to determine the unbalance. Therefore, a rigid body model of the rotor can be used. Experiences with the KIS system have shown that the housing can have a strong influence on the vibrational behaviour due to unbalances. Hence, the rotordynamic model used in this paper additionally includes an elastically suspended rigid housing. In the first step, the equations of motion for one bearing plane are given. With this model the basic behaviour is discussed. In a second step the equations of motion for the complete model are given. Measurements and simulation results are shown for this two plane model.

2 One Plane Rotor Dynamic Model

The motion of a rotating rotor due to the rotational synchronous unbalance excitation is rotationally sychronous itself. The orbit is circular with ideal isotropic suspension or elliptical with anisotropic suspension (see also [Kel87]). Magnetic suspension itself can be considered isotropic whereas the housing suspension can cause anisotropy. In this paper isotropic suspension is assumed.

Harmonic vibrations can be described by complex variables. Time functions $f(t) = a\cos(\Omega t) + b\sin(\Omega t)$ can be transformed to complex time functions $\boldsymbol{f}(t) = (a - jb)e^{j\Omega t} = \boldsymbol{c}e^{j\Omega t}$ (see also [Mar86]).

The complex motion variables in equation 1 represent the motion in x- and y-direction. This can also be seen in figure 2.

$$\boldsymbol{x}_e = r_e e^{j\varphi_e}, \boldsymbol{x}_r = r_r e^{j\varphi_r}, \boldsymbol{x}_g = r_g e^{j\varphi_g} \tag{1}$$

The equations of motion of the rotor and the housing ($\boldsymbol{i} = i_x - j i_y$) are:

$$m_r\left(\ddot{\boldsymbol{x}}_e + \ddot{\boldsymbol{x}}_r + \ddot{\boldsymbol{x}}_g\right) = k_s\boldsymbol{x}_r + k_i\boldsymbol{i} \tag{2}$$

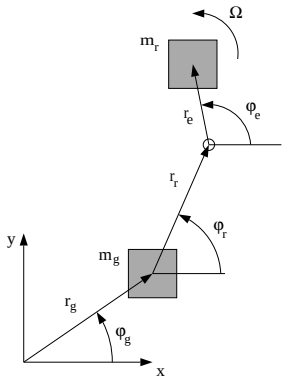

Figure 2: Two mass model for one bearing plane.

$$m_g\ddot{\boldsymbol{x}}_g = -k_s\boldsymbol{x}_r - k_i\boldsymbol{i} - d_g\dot{\boldsymbol{x}}_g - k_g\boldsymbol{x}_g \tag{3}$$

Using complex time functions the differential operator $\partial/\partial t$ can be replaced by $j\Omega$ and equations 2 and 3 are then transformed to:

$$-m_r\Omega^2\left(\boldsymbol{x}_e + \boldsymbol{x}_r + \boldsymbol{x}_g\right) = k_s\boldsymbol{x}_r + k_i\boldsymbol{i} \tag{4}$$

$$-m_g\Omega^2\boldsymbol{x}_g = -k_s\boldsymbol{x}_r - k_i\boldsymbol{i} - d_g j\Omega\boldsymbol{x}_g - k_g\boldsymbol{x}_g \tag{5}$$

From equations 4 and 5 the eccentricity $\boldsymbol{x}_e$ can be calculated.

$$\boldsymbol{x}_e = -\boldsymbol{x}_r - \frac{\tilde{k}_s}{m_r\Omega^2}\boldsymbol{x}_r - \frac{\tilde{k}_i}{m_r\Omega^2}\boldsymbol{i} \tag{6}$$

For simplicity the influence of an elastically suspended housing can be modelled with magnetic bearing parameters k_s and k_i which depend on the rotational speed. These parameters are named $\tilde{k}_s$ and $\tilde{k}_i$ and are given in equations 7 and 8.

In case of negligible influence of the housing, $\tilde{k}_s$ can be replaced by ${k_s}^2$. Figure 3 shows the behavior of the normalized force-displacement factor $\tilde{k}_s/k_s$. Three frequency ranges can be distinguished. At low rotational speed $\tilde{k}_s \approx k_s$ and at high rotational speed $\tilde{k}_s \approx k_s\frac{m_r}{m_g}$. The transition range is characterized by a resonance where the amplitude first decreases and then increases and a phase shifts up to 180° occurs.

$$\tilde{k}_s = k_s + \frac{m_r\Omega^2}{m_g\Omega^2 - d_g j\Omega - k_g}k_s \tag{7}$$

$$\tilde{k}_i = k_i + \frac{m_r\Omega^2}{m_g\Omega^2 - d_g j\Omega - k_g}k_i \tag{8}$$

With known housing influence ($\tilde{k}_s$, $\tilde{k}_i$) and measured position x_r and current i, the eccentricity can be evaluated

[2] The characteristics of k_s and k_i are similar. Therefore, only k_s is discussed here.

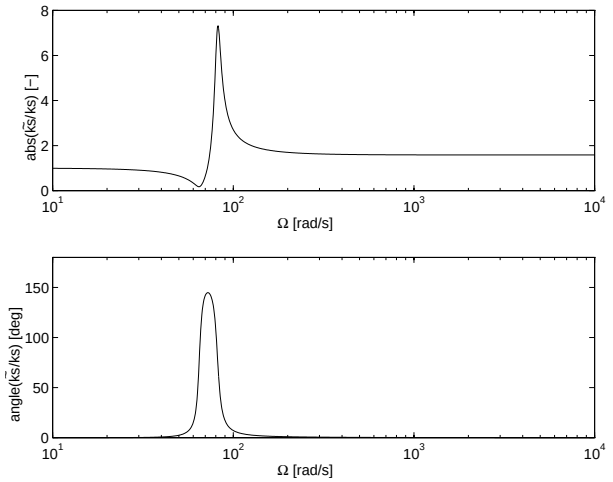

Figure 3: Normalized force-displacement factor $\tilde{k}_s/k_s$ or $\tilde{k}_i/k_i$ depending on the rotational speed Ω.

by equation 6. With the evaluated eccentricity the rotor can be balanced with an additional balancing mass $\Delta m\boldsymbol{r} = -m_r\boldsymbol{x}_e$, where $\boldsymbol{r}$ represents the radius and the orientation of the balancing mass Δm.

3 Two Plane Rotor Dynamic Model

The one bearing plane model introduced in the previous section can show the basic behaviour of a rotor with an unbalance. Nevertheless, a complete model is necessary for balancing and for the estimation of the unbalance compensation parameters. The mechanical model has to include the geometric and dynamic coupling of the bearing planes caused by the mass distribution of the rotor and by the gyroscopic effects.

In the first step the equations of motion are derived at the centres of gravity. In the second step these equations of motion are transformed into the coordinates of the two bearing planes.

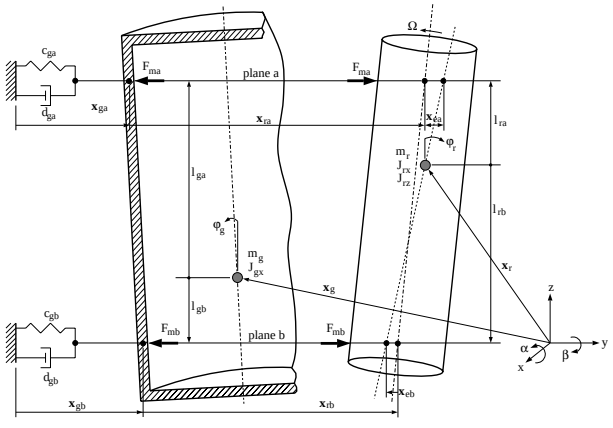

Figure 4: rotor and housing model for two bearing planes.

$$\boldsymbol{F}_{ma} = k_{sa}\boldsymbol{x}_{ra} + k_{ia}\boldsymbol{i}_a \tag{9}$$

$$\boldsymbol{F}_{mb} = k_{sb}\boldsymbol{x}_{rb} + k_{ib}\boldsymbol{i}_b \tag{10}$$

$$\boldsymbol{F}_{ga} = k_{ga}\boldsymbol{x}_{ga} + d_{ga}\dot{\boldsymbol{x}}_{ga} \tag{11}$$

$$\boldsymbol{F}_{gb} = k_{gb}\boldsymbol{x}_{gb} + d_{gb}\dot{\boldsymbol{x}}_{gb} \tag{12}$$

The equations of motion (formulated at the centres of gravity) of the rotor and the housing:

$$m_r\ddot{\boldsymbol{x}}_r = \boldsymbol{F}_{ma} + \boldsymbol{F}_{mb} \tag{13}$$

$$m_g\ddot{\boldsymbol{x}}_g = -\boldsymbol{F}_{ma} - \boldsymbol{F}_{mb} - \boldsymbol{F}_{ga} - \boldsymbol{F}_{gb} \tag{14}$$

$$J_{rx}\ddot{\boldsymbol{\varphi}}_r - j\Omega J_{rz}\dot{\boldsymbol{\varphi}}_r = l_{ra}\boldsymbol{F}_{ma} + l_{rb}\boldsymbol{F}_{mb} \tag{15}$$

$$J_{gx}\ddot{\boldsymbol{\varphi}}_g = -l_{ga}(\boldsymbol{F}_{ma} + \boldsymbol{F}_{ga}) - l_{gb}(\boldsymbol{F}_{mb} + \boldsymbol{F}_{gb}) \tag{16}$$

The transformation to the bearing plane coordinates is given by:

$$\begin{bmatrix} \boldsymbol{x}_{ea} + \boldsymbol{x}_{ra} + \boldsymbol{x}_{ga} \\ \boldsymbol{x}_{eb} + \boldsymbol{x}_{rb} + \boldsymbol{x}_{gb} \end{bmatrix} = \begin{bmatrix} 1 & -jl_{ra} \\ 1 & -jl_{rb} \end{bmatrix} \begin{bmatrix} \boldsymbol{x}_r \\ \boldsymbol{\varphi}_r \end{bmatrix} \tag{17}$$

$$\begin{bmatrix} \boldsymbol{x}_{ga} \\ \boldsymbol{x}_{gb} \end{bmatrix} = \begin{bmatrix} 1 & -jl_{ga} \\ 1 & -jl_{gb} \end{bmatrix} \begin{bmatrix} \boldsymbol{x}_g \\ \boldsymbol{\varphi}_g \end{bmatrix} \tag{18}$$

Here, $\boldsymbol{\varphi}_r = \alpha_r + j\beta_r$ and $\boldsymbol{\varphi}_g = \alpha_g + j\beta_g$.

Combining equations 9 - 18 leads to:

$$\begin{aligned} \boldsymbol{M}_r \begin{bmatrix} \ddot{\boldsymbol{x}}_{ea} + \ddot{\boldsymbol{x}}_{ra} + \ddot{\boldsymbol{x}}_{ga} \\ \ddot{\boldsymbol{x}}_{eb} + \ddot{\boldsymbol{x}}_{rb} + \ddot{\boldsymbol{x}}_{gb} \end{bmatrix} &= \boldsymbol{K}_s \begin{bmatrix} \boldsymbol{x}_{ra} \\ \boldsymbol{x}_{rb} \end{bmatrix} \\ &+ \boldsymbol{K}_i \begin{bmatrix} \boldsymbol{i}_a \\ \boldsymbol{i}_b \end{bmatrix} \end{aligned} \tag{19}$$

$$\begin{aligned} \boldsymbol{M}_g \begin{bmatrix} \ddot{\boldsymbol{x}}_{ga} \\ \ddot{\boldsymbol{x}}_{gb} \end{bmatrix} &= -\boldsymbol{K}_s \begin{bmatrix} \boldsymbol{x}_{ra} \\ \boldsymbol{x}_{rb} \end{bmatrix} - \boldsymbol{K}_i \begin{bmatrix} \boldsymbol{i}_a \\ \boldsymbol{i}_b \end{bmatrix} \\ &- \boldsymbol{D}_g \begin{bmatrix} \dot{\boldsymbol{x}}_{ga} \\ \dot{\boldsymbol{x}}_{gb} \end{bmatrix} - \boldsymbol{K}_g \begin{bmatrix} \boldsymbol{x}_{ga} \\ \boldsymbol{x}_{gb} \end{bmatrix} \end{aligned} \tag{20}$$

The mass matrices of equations 19 and 20 are given by:

$$\boldsymbol{M}_r = \frac{1}{l^2}\left(J_{rx} - J_{rz} + m_r \begin{bmatrix} l_{rb}^2 & l_{ra}l_{rb} \\ l_{ra}l_{rb} & l_{ra}^2 \end{bmatrix}\right) \tag{21}$$

$$\boldsymbol{M}_g = \frac{1}{l^2}\left(J_{gx} + m_g \begin{bmatrix} l_{gb}^2 & l_{ga}l_{gb} \\ l_{ga}l_{gb} & l_{ga}^2 \end{bmatrix}\right) \tag{22}$$

with $l = l_{ra} - l_{rb} = l_{ga} - l_{gb}$. The stiffness and damping parameters of the rotor and housing remain unchanged, e.g. the matrices $\boldsymbol{K}_s$, $\boldsymbol{K}_i$, $\boldsymbol{K}_g$ and $\boldsymbol{D}_g$ are diagonal and

the diagonal elements remain unchanged (isotropic bearing and housing).

$$\boldsymbol{K}_s = \begin{bmatrix} k_{sa} & 0 \\ 0 & k_{sb} \end{bmatrix}, \boldsymbol{K}_i = \begin{bmatrix} k_{ia} & 0 \\ 0 & k_{ib} \end{bmatrix} \tag{23}$$

$$\boldsymbol{K}_g = \begin{bmatrix} k_{ga} & 0 \\ 0 & k_{gb} \end{bmatrix}, \boldsymbol{D}_g = \begin{bmatrix} d_{ga} & 0 \\ 0 & d_{gb} \end{bmatrix} \tag{24}$$

Equation 19 and 20 can be transformed to:

$$\begin{aligned} \begin{bmatrix} \boldsymbol{x}_{ea} \\ \boldsymbol{x}_{eb} \end{bmatrix} &= -\begin{bmatrix} \boldsymbol{x}_{ra} \\ \boldsymbol{x}_{rb} \end{bmatrix} - \left(\boldsymbol{M}_r\Omega^2\right)^{-1} \tilde{\boldsymbol{K}}_s \begin{bmatrix} \boldsymbol{x}_{ra} \\ \boldsymbol{x}_{rb} \end{bmatrix} \\ &\quad - \left(\boldsymbol{M}_r\Omega^2\right)^{-1} \tilde{\boldsymbol{K}}_i \begin{bmatrix} \boldsymbol{i}_a \\ \boldsymbol{i}_b \end{bmatrix} \end{aligned} \tag{25}$$

with:

$$\tilde{\boldsymbol{K}}_s = \boldsymbol{K}_s + \boldsymbol{M}_r\Omega^2 \left(\boldsymbol{M}_g\Omega^2 - j\Omega\boldsymbol{D}_g - \boldsymbol{K}_g\right)^{-1} \boldsymbol{K}_s \tag{26}$$

$$\tilde{\boldsymbol{K}}_i = \boldsymbol{K}_i + \boldsymbol{M}_r\Omega^2 \left(\boldsymbol{M}_g\Omega^2 - j\Omega\boldsymbol{D}_g - \boldsymbol{K}_g\right)^{-1} \boldsymbol{K}_i \tag{27}$$

The structure of the equations for the one plane model remains the same as for the two plane model while the order is increased. The variables are replaced by vectors and the parameters are replaced by matrices. The coupling of the bearing planes is given by the outer diagonal elements of the mass matrices $\boldsymbol{M}_r$ and $\boldsymbol{M}_g$.

The balancing of a ridig rotor is carried out by adding two balancing masses Δm_a and Δm_b and using two balancing planes with radius and orientation $\boldsymbol{r}_a$ and $\boldsymbol{r}_b$. For simplicity the balancing planes are chosen to be identical to the magnetic bearing planes. In practice the balancing must be done somewhere else and the balancing masses have to be transformed into new planes (see [Kel87]).

$$\begin{bmatrix} \Delta m_a \boldsymbol{r}_a \\ \Delta m_b \boldsymbol{r}_b \end{bmatrix} = -\boldsymbol{M}_r \begin{bmatrix} \boldsymbol{x}_{ea} \\ \boldsymbol{x}_{eb} \end{bmatrix} \tag{28}$$

4 Unbalance Compensation

The reference position of the magnetic bearing controller is the geometric axis of the rotor. The unbalance of a rotor causes rotational synchronous harmonic unbalance forces which increase with the square of the rotational speed. These unbalance forces cause rotational synchronous harmonic forces in the bearings which may lead to current saturation of the amplifiers. Therefore, any unbalance can limit the maximum rotational speed. Furthermore, these unbalance forces cause undesirable housing vibrations.

Unbalance compensation[3] is a well-known technique for magnetic bearing systems (see [HB84], [KTF95], [HOM92], [LH94]). The goal is to reduce the rotational synchronous current components of the magnetic bearings to zero. The reference position of the magnetic bearing controller is now chosen adaptively so that no rotational synchronous controller forces are generated in the bearings. Nevertheless, the rotor does not, as often written, rotate in a "force-free" manner due to the residual bearing forces resulting from the negative magnetic bearing stiffness. Moreover, due to these forces the rotor does not spin about its principal axis of inertia but about an axis which is between its geometrical axis and its principal axis of inertia. Figure 6 shows that, for high rotational speed, the principal axis of inertia is the limiting value of the spinning axis. The residual bearing forces described above are small and their influence decreases with rotational speed, so that with unbalance compensation, both magnetic bearing forces and housing vibrations can be greatly reduced.

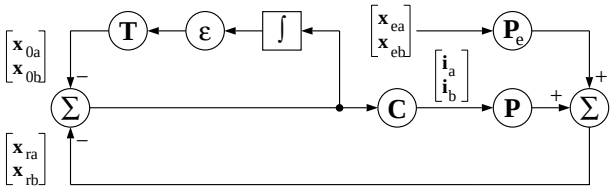

Figure 5: Structure of a magnetic bearing system with unbalance compensation.

Figure 5 shows a possible implementation of a magnetic bearing system with unbalance compensation. In addition to the magnetic bearing controller $\boldsymbol{C}$ a superposed control loop is used which adds rotational synchronous signals ($\boldsymbol{x}_{0a}$ and $\boldsymbol{x}_{0b}$) to the measured positional signals ($\boldsymbol{x}_{ra}$ and $\boldsymbol{x}_{rb}$). When the adaptation of unbalance compensation is complete, the rotational synchronous controller input is zero. Hence the rotational synchronous controller output, i.e. the rotational synchronous current, is zero.

From equation 25 the plant descriptions $\boldsymbol{P}$ and $\boldsymbol{P}_e$ can be identified.

$$\boldsymbol{P} = -\left(\boldsymbol{M}_r\Omega^2 + \tilde{\boldsymbol{K}}_s\right)^{-1} \tilde{\boldsymbol{K}}_i \tag{29}$$

$$\boldsymbol{P}_e = -\left(\boldsymbol{M}_r\Omega^2 + \tilde{\boldsymbol{K}}_s\right)^{-1} \boldsymbol{M}_r\Omega^2 \tag{30}$$

The rotor diplacement with unbalance compensation switched on is given by:

$$\begin{bmatrix} \boldsymbol{x}_{ra} \\ \boldsymbol{x}_{rb} \end{bmatrix} = \boldsymbol{P}_e \begin{bmatrix} \boldsymbol{x}_{ea} \\ \boldsymbol{x}_{eb} \end{bmatrix} \tag{31}$$

[3]The term "unbalance compensation" is somehow misleading because neither the unbalance nor the unbalance forces are compensated.

Figure 6 shows a plot of the rotor displacement as a function of the rotational speed with and without unbalance compensation (one plane model). The influence of the housing is neglected. It can be seen, that the rotor displacement $\boldsymbol{x}_r$ for high rotational speed is the opposite of the eccentricity $\boldsymbol{x}_e$. Therefore, the rotor rotates about its principal axis of inertia.

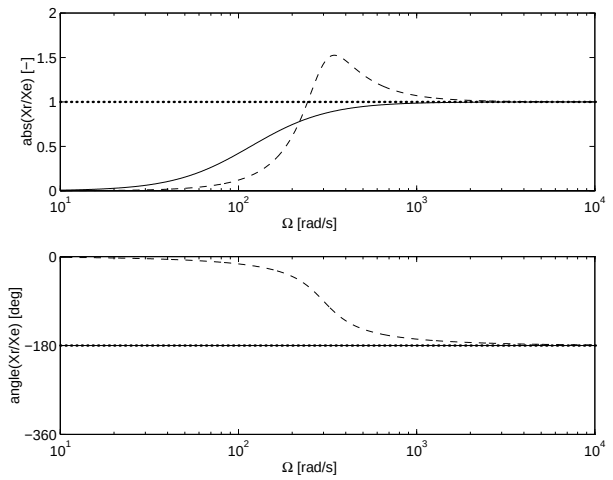

Figure 6: Normalized rotor displacement $\boldsymbol{x}_r/\boldsymbol{x}_e$ depending on the rotational speed Ω (solid line: with unbalance compensation, dashed line: without unbalance compensation).

The dynamics of the superposed control loop, adjustable by ε, are much slower than the dynamics of the magnetic bearing control and, therefore, do not affec the positional controller of the magnetic bearing (see also [HBGL96]). $\boldsymbol{P}$ is the plant of the magnetic bearing system and $\boldsymbol{P}_e$ is the plant of unbalance (disturbance force input). $\boldsymbol{T}$ is a complex linearisation factor which can be chosen to be the inverse of the sensitivity function $\boldsymbol{T} = \boldsymbol{S}^{-1} = \boldsymbol{I} + \boldsymbol{PC}$ due to the fact that the unbalance compensation dynamics of all radial degrees of freedom is then equal. If $\boldsymbol{T}$ is chosen different from $\boldsymbol{S}^{-1}$, overshoot or even instability can occur when unbalance compensation is started. More information about the transient behaviour of unbalance compensation can be found in [Ahr96].

5 Balancing With Magnetic Bearing Data

In order to achieve good balancing data, the system parameters k_s, k_i, d_g and k_g have to be known sufficiently. The influence of k_i can be eliminated for measurements with unbalance compensation. Here the rotational synchronous component of the current is zero.

From equation 6 it can be seen that the rotor displacement $\boldsymbol{x}_r$ converges to $-\boldsymbol{x}_e$ with increasing rotational speed. This behaviour is independent of the use of unbalance compensation. Therefore, the infuence of the parameters mentioned above decreases with increasing rotational speed.

The KIS rotor was unbalanced to such an extent, that the eccentricity exceeded the air gap of the magnetic bearings. Due to this high level of unbalance current saturation of the magnetic bearings occured and, therefore, limited the rotational speed. It is clear that unbalance compensation can only be used when the resulting diplacement does not exceed the air gap. Therefore, equation 25 has to be used for balancing. An additional problem is the fact that the identification of k_s and k_i depends on the housing suspension [Ahr96]. Moreover, the measured data greatly depends on the housing dynamics and the magnetic bearing parameters. In order to overcome these problems and to achieve sufficient balancing data test unbalance masses have been used. With these measurements initial balancing was possible which reduced the unbalance of the rotor significantly and allowed the usage of unbalance compensation at higher rotational speed. This iterative balancing process led to good results.

6 Open-loop Resonance of the Nutation Mode

The denominator *den* of equation 29 or 30 (housing dynamics neglected) determines the rotor motion with unbalance compensation (equation 31) in a crucial way. This denominator can be expressed as follows:

$$\begin{aligned} den(\Omega) &= m_r\,(J_x - J_z)\,\Omega^4 \\ &+ \left(\frac{m_r}{2}k_s l^2 + 2k_s\,(J_x - J_z)\right)\Omega^2 \\ &+ k_s^2 l^2 \end{aligned} \tag{32}$$

For simplicity $k_{sa} = k_{sb} = k_s$, $l_a = l/2$ and $l_b = -l/2$ have been chosen. In this case translational and angular modes can be decomposed and the basic behaviour can be discussed in an easier way. More detailed information can be found in [Ahr96].

In equation 32 it can be seen that for $J_x > J_z$ there are no real solutions for Ω when $den = 0$. For $J_x < J_z$, however, a real solution for Ω can be found. At this rotational speed, the system with unbalance compensation (equation 31) has a resonance. The resonance frequency Ω_{res} is

$$\Omega_{res} = \sqrt{\frac{k_s l^2}{2\,(J_z - J_x)}}. \tag{33}$$

If $J_z > J_x$, i.e. for highly gyroscopic systems, the nutation mode becomes unstable at the resonance frequency Ω_{res}. This resonance frequency depends on the ratio of moments of inertia J_z/J_x and occurs for all ratios which are physically possible. Ω_{res} varies from $\sqrt{\frac{k_s l^2}{2J_x}}$ for $J_z = 2J_x$ to ∞ for $J_z = J_x$. Therefore, this behaviour has to be considered in the design of magnetically suspended flywheels or other highly gyroscopic rotors where the ratio of the moments of inertia $J_z/J_x \geq 1$.

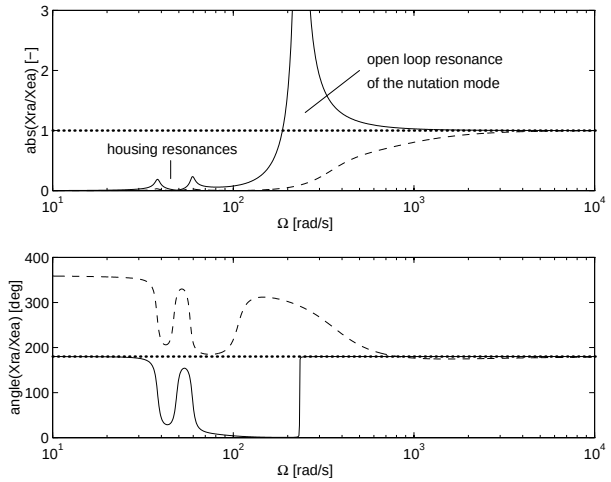

Figure 7: Normalized rotor displacement $\boldsymbol{x}_{ra}/\boldsymbol{x}_{ea}$ of one bearing plane as function of the rotor speed Ω (solid line: with unbalance compensation, dashed line: without unbalance compensation).

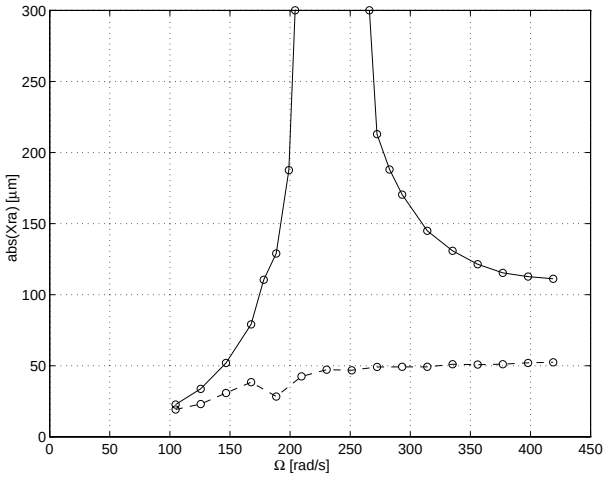

Figure 8: Measured rotor displacement $\boldsymbol{x}_{ra}$ of one bearing plane as function of the rotor speed Ω (upper line: with unbalance compensation, lower line: without unbalance compensation).

7 Summary

The basic behaviour of a highly unbalanced rotor with magnetic suspension has been shown. The unbalance forces in the bearing may lead to current saturation and, therefore, limit the rotational speed. It has been shown that balancing can be achieved using the data obtained from the magnetic bearing system. The influence of the housing dynamics has been analyzed. Experiences with unbalance compensation have been given and a resonance phenomena for unbalance compensation has been shown. This resonance is crucial for magnetic bearing systems with high gyroscopic coupling when unbalance compensation is used.

References

[Ahr96] M. Ahrens. *Zur magnetischen Lagerung von Schwungrad-Energiespeichern.* PhD thesis, ETH Eidgenössische Technische Hochschule, to appear 1996.

[HB84] H. Habermann and M. Brunet. The Active Magnetic Bearing Enables Optimum Damping of Flexible Rotors. In *ASME International Gas Turbine Conference*, Amsterdam, 1984.

[HBGL96] R. Herzog, P. Bühler, C. Gähler, and R. Larsonneur. Unbalance Compensation Using Generalized Notch Filters in the Multivariable Feedback of Magnetic Bearings. *IEEE Transactions on Control Systems and Technology, Special Issue on Magnetic Bearing Systems*, 1996.

[HOM92] T. Higuchi, M. Otsuka, and T. Mizuno. Identification of Rotor Unbalance and Reduction of Housing Vibrations by Periodic Learning Control in Magnetic Bearings. In *3rd International Symposium on Magnetic Bearings*, Washington, 1992.

[Kel87] W. Kellenberger. *Elastisches Wuchten.* Springer-Verlag, Berlin, 1987.

[KTF95] C. Knospe, S. Tamir, and S. Fedigan. Design of Robust Adaptive Unbalance Response Controllers for Rotors With Magnetic Bearings. In *3rd International Symposium on Magnetic Suspension Technology*, Tallahassee, 1995.

[LH94] R. Larsonneur and R. Herzog. Feedforward Compensation of Unbalance: New Results and Application Experiences. In *IUTAM Symposium The Active Control of Vibration*, Bath, 1994.

[Mag71] K. Magnus. *Kreisel, Theorie und Anwendungen.* Springer-Verlag, Berlin, 1971.

[Mar86] H. Marko. *Methoden der Systemtheorie.* Springer-Verlag, Berlin, 1986.